A Novel Fault Localization Technique for PV Systems Using a Single-Voltage Sensor

Ali Alhejab, *Student Member, IEEE,* Muhammad Abbasi, Shehab Ahmed, *Senior Member, IEEE,*

***Abstract*—Photovoltaic (PV) systems are gaining popularity as a source of sustainable energy, however, undiscovered faults within these systems may cause significant efficiency reduction. Localizing these faults to the module level is important for a quick fault diagnosis and maintaining the overall system efficiency. This paper presents a new method for localizing line-to-line, line-to-ground, inter-string, partial shading, and open-circuit faults in an N by M PV array down to the module level. The approach utilizes a single voltage sensor and $\lceil N/2 \rceil$ switches to control the connected PV modules. The technique initially relies on identifying the faulty string, and once this string is determined, the voltage associated with each module in that string is found. Each module voltage in that string is obtained by measuring the string voltage after bypassing each module corresponding to an activated switch. Subsequently, the resulting linear equations are solved to obtain the voltage of each module in that faulty string. The technique is verfied using simulation, and expiremental setup for a 5 by 4 small-size PV system. Experimental and simulation results demonstrate that the technique can accurately localize faulty modules with only N voltage samples of the faulty string.**

***Index Terms*—Photovoltaic (PV) array, Moving Average, Fault Detection, Module Level, Single Sensor, Fault Localization, Open Fault, Short Fault.**

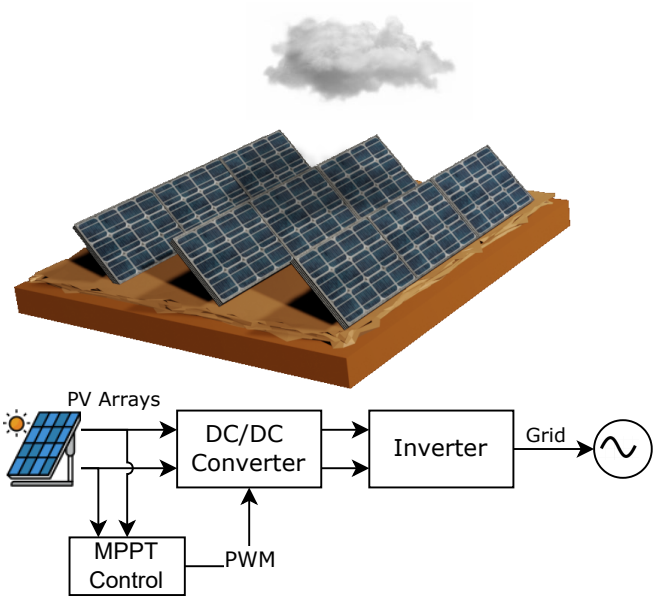

Fig. 1. Photovoltiac (PV) Power System

I. Introduction

PHOTOVOLTAIC (PV) systems are becoming more popular as a clean energy source, however, the susceptibility of these systems to faults can result in a significant drop in efficiency or even fire hazards [1]. Hence, developing fault detection and localization techniques is essential to prevent permanent damage to the energy system.

In the litrature, various techniques are used for PV fault detection, and localization including visual inspection [2]–[4], infrared thermography [5]–[13] , and electroluminescence [14]–[20]. However, each of these techniques is either complex to implement, requires expensive additional equipment for monitoring, or irradiance dependent which may not be practical for large-scale PV systems.

An irradiance-independent fault detection, and localization technique based on Spread Spectrum Time-Domain Reflectometry (TDR) is introduced in [21], however, it can only localize line-to-ground, and open-string faults. In [22]–[24], another irradiance-independent voltage-based localization technique is shown; nevertheless, to precisely localize the fault location to the module level, a voltage sensor is required for each module.

Ali Alhejab, Muhammad Abbasi, and Shehab Ahmed are with the Computer, Electrical, and Mathematical Sciences and Engineering Division, King Abdullah University of Science and Technology, Thuwal 23955-6900, Saudi Arabia (e-mail: ali.hejab@kaust.edu.sa; muhammad.abbasi@kaust.edu.sa ;shehab.ahmed@kaust.edu.sa).

The work in [25]–[28] minimizes the number of sensors required to locate faults by optimizing the locations of these sensors such that the voltage of each module can be obtained mathematically. Moreover, to reduce the number of voltage sensors, the study in [29] employed one diode per string and a single voltage sensor to determine the number of faulty modules and the string in which they occurred. However, this approach does not show the exact location of the faulty module, and only identify the location at which the string at is faulty. Furthermore, in [30], a single voltage sensor referenced to ground along with a switch attached to each module such that the voltage of each module can is obtained by connecting each module at a time to the multimeter. Nevertheless, this work does not optimise the number of switches per string, and requires extra connection for each module.

In this work, a technique to reduce the number of voltage sensors to one and minimizes the number of switches required to precisely localize the faulty modules of the PV string is introduced. The paper is structured into four sections: Section II covers PV Modeling and Fault Characteristics, Section III discusses the Fault Detection and Localization Algorithm, Section IV presents Simulation Results, Section V shows Experimental Results, and Section VI concludes the study.

II. PV Modeling, and Faults

A. Modeling

Modeling the PV system is necessary to understand the system response during fault. The simplest model for a PV cell is the single-diode model shown in Fig. 2.

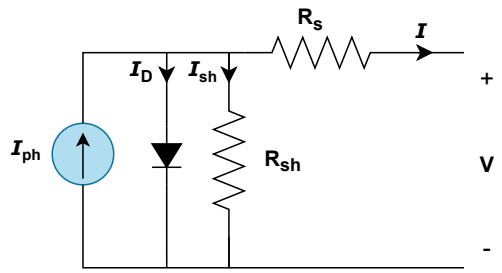

Fig. 2. Single Diode Model

The PV cell behavior can be described with the following equation:

$$I = I_{ph} - \underbrace{I_o\left(\exp\left(\frac{V+IR_s}{nV_T}\right)-1\right)}_{I_D} - \underbrace{\frac{V+IR_s}{R_{sh}}}_{I_{sh}} \quad (1)$$

Where V is the voltage generated by the PV cell, I the cell output current, I_{ph} photo-current controlled by light intensity, I_0 reverse saturation current , R_s series resistance to represent the losses, R_{sh} shunt resistance to represents the leakage, n the ideality factor, and V_t is the thermal voltage. A higher light intensity increases the current output of the cell, while a decrease in temperature increases the cell voltage, and hence a rise in power in both cases. Therefore, numerous fault detection algorithms necessitate the use of extra sensors for temperature or light intensity, as these variables can significantly affect the power output of the PV system, as shown in (1), and assist in identifying faults.

B. PV Faults

The current and voltage behavior of the PV system is dependent on the type of fault the system experiences. The common types of faults in PV systems are open, short, inter-string, and partial shading faults.

1) Partial Shading Fault: Partial shading is the case where the irradiance over a segment of the PV system is not uniformly distributed, resulting in a power mismatch and an overall decrease in the PV system performance. Although shading a module can result in a current reduction, bypass diodes overcome this by shorting the shaded module, and hence causing a reduction in voltage rather than affecting the full string performance.

2) Open Circuit Fault: The open circuit fault results from a disconnection in the string. This disconnection in the circuit can be bypassed by the diode, similar to the case of partial shading. However, in case the open circuit is after the bypass diode, a full string loss may occurs.

3) Line to Line Fault: A line-to-line fault is the result of an unintended connection between two terminals, leading to the shorting of all modules in between these two terminals. This fault can cause permanent damage or even a fire in the system. Two special cases of this fault are the line-to-ground and inter-string fault. In the inter-string fault, an unintended connection between two strings results in a voltage mismatch and, hence, a power drop. However, in the line-to-ground fault, non-current-carrying conductors, such as PV mounting racks and PV module frames, come into contact with a current-carrying conductor. This fault would result in a chain of modules having a voltage close to zero.

4) Faults I-V Characteristics: Fig. 3 shows the I-V behavior of the PV system under various types of faults. It can be seen that an open string results in a current drop, while a short fault leads to a voltage drop. In the case of partial shading, either a current or voltage drop may occur, depending on the Maximum Power Point Tracking (MPPT) algorithm and the location of the Global Maximum Power Point (GMPP).

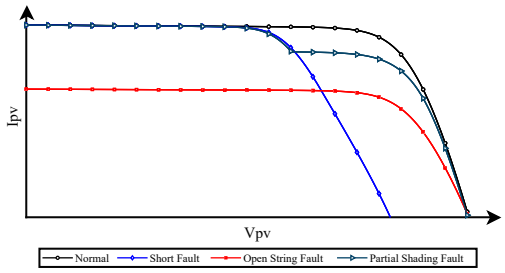

(a) Current Curves During Fault

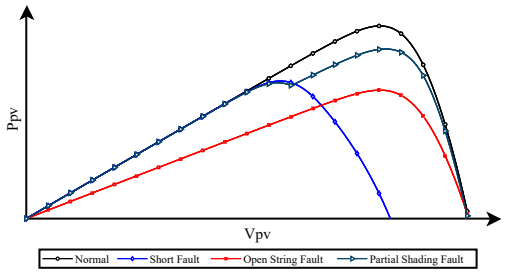

(b) Power Curves During Fault

Fig. 3. IV Curve Response to Various Fault Conditions

This work only focuses on faults that reduces the voltage level of the system. Faults that do not activate the bypass diode or cause a module voltage drop are not considered. In the next section, the proposed fault detection and localization algorithm is discussed.

III. Fault Localization Algorithm

This section discusses the proposed fault detection, and localization algorithm. The method can detect and localize partial shading, short, and open faults to the module level. Fig. 4 shows the general structure for PV system where the proposed algorithm can be used to localize faults to the module level. The fusion center samples the data of the PV string to

identify which string underperforms compared to the other strings. In an ideal scenario, the voltage across all strings should be equal. A faulty string, as demonstrated in Fig. 3, exhibits a drop in voltage once a fault occurs, aiding in its localization. Switches are connected to each string to serve as bypass paths, allowing control over which set of modules are connected to the faulty string. The voltage of that faulty string is sampled with every switch combination, such that the module's voltages can be obtained mathematically.

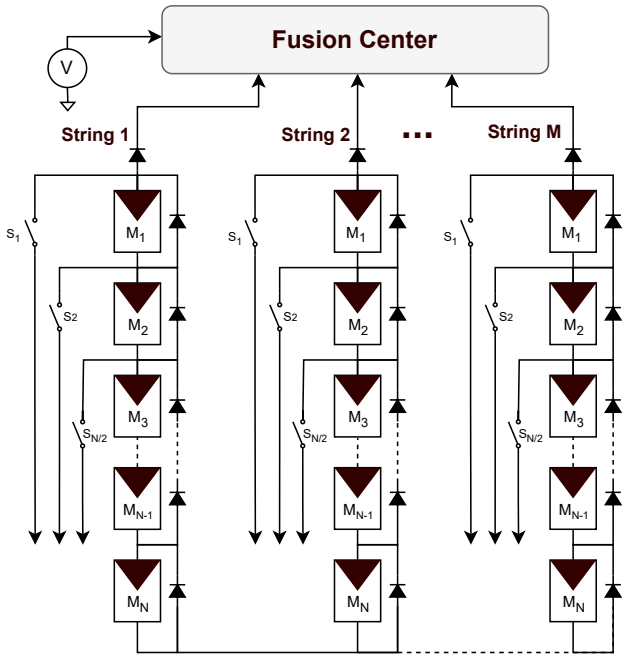

Fig. 4. General Structure of PV System with Fault Localization Switches

A. String Fault Localization

As discussed earlier, to localize the fault to the module level, the string must be localized first. This section shows a simple string localization technique that is used in this study. Other techniques are thoroughly discussed in [23], [24]. The algorithm starts by sequentially sampling each string to create a vector $\mathbf{V}$ that contains the voltage of each string:

$$\mathbf{Vs} = [Vs_0, Vs_1, \ldots, Vs_n] \tag{2}$$

The vector $\mathbf{V}$ is then used to find the maximum voltage of all strings denoted as V_m. This maximum value is then utilized in a moving average model, which predicts the voltage for the following time step as follows:

$$V_p(t+1) = \alpha V_m(t) + (1-\alpha)V_p(t) \tag{3}$$

Here, V_p represents the predicted voltage, and α is a decay factor. This step is important because during a fault, such as a line-to-ground, all strings may go to zero. Therefore, employing a moving average that tracks only the maximum string voltage can help in detecting extreme fault scenarios. Next, the vector $\mathbf{V}$ is compared with the predicted voltage value V_p to find deviation ratio vector such that

$$\epsilon = \left| \frac{\mathbf{Vs}(t+1) - V_p(t)}{V_p(t)} \right| \tag{4}$$

The deviation ratio vector, denoted as ϵ, helps in identifying faulty strings. If a string exhibits a deviation ratio exceeding a predefined threshold, it is labeled as faulty. Algorithm. 1 shows a step-by-step procedure for the discussed string fault localization technique.

Algorithm 1 String Fault Localization Algorithm

Initialization: Decay factor α, empty sets $\mathbf{Vs}$, and $\mathbf{S}$.
for i from 1 to M **do**
  Measure Vs_i
  Assign $\mathbf{Vs(i)}$ to Vs_i.
end for
Assign Vm to max($\mathbf{Vs}$).
Predict V_p using (3)
Calculate ϵ from (4)
for j from 1 to M **do**
  if $\epsilon\ (j) >$ threshould **then**
    Add j to set S.
  end if
end for
Output: Set S as the indices of faulty strings.

Once the faulty string is localized, switches can be used to identify the faulty module as discussed in the next subsection.

B. Module Fault Localization

The set of switches attached to each string, shown in Fig 4, serve the purpose of bypassing each module in the localized faulty string. By bypassing these modules and sensing the voltage after each switch combination, a system of linear equations is created. To generate a system of N equations, for a string of N modules, $\lceil N/2 \rceil$ switches are needed. The resulting equations from controlling these switches can be represented as follows:

$$V_{pv} = A\mathbf{V} \tag{5}$$

Where $\mathbf{Vpv}$ represents the string voltage for each switch combination:

$$\mathbf{V_{pv}} = \begin{bmatrix} V_{pv0} \\ V_{pv1} \\ V_{pv2} \\ \vdots \end{bmatrix} \tag{6}$$

$\mathbf{A}$ is the voltage coefficient matrix for the active modules due to each switch combination:

$$\mathbf{A} = \begin{bmatrix} a_{00} & a_{01} & a_{02} & \vdots \\ a_{10} & a_{11} & a_{12} & \vdots \\ a_{20} & a_{21} & a_{22} & \vdots \\ \vdots & \vdots & \vdots & \vdots \end{bmatrix} \tag{7}$$

and $\mathbf{V}$ is the voltage of each module:

$$\mathbf{V} = \begin{bmatrix} V_0 \\ V_1 \\ V_2 \\ \vdots \end{bmatrix} \tag{8}$$

Once the set of linear equations for the system are represented in their matrix form, the linear system can be solved to obtain the voltage for each module. To illustrate, consider a faulty string of five series modules, similar to the one shown in Fig. 5.

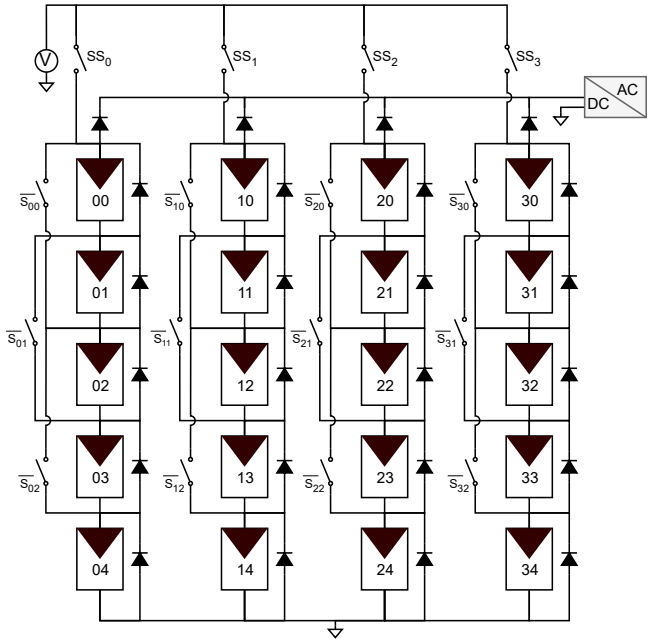

Fig. 5. Layout of the Simulated 5x4 PV System

Table. I shows the linear equations corresponding to the activation of each switch combination in a faulty string of five modules.

TABLE I
VPV VOLTAGES FOR DIFFERENT SWITCH COMBINATIONS

$\mathbf{V_{pv}}$	Switch Combination	Linear Equation
V_{pv0}	S0=1, S1=S2=0	$V_0 + V_4$
V_{pv1}	S3=1, S2=S3=0	$V_3 + V_4$
V_{pv2}	S2=1, S1=S3=0	V_4
V_{pv3}	S2=S3=1, S1=0	$V_2 + V_3 + V_4$
V_{pv4}	S1=S2=1, S3=0	$V_0 + V_1 + V_4$

The matrix form for the set of equations resulting from activating the different switch combinations is shown in Table. I:

$$\begin{bmatrix} V_{pv0} \\ V_{pv1} \\ V_{pv2} \\ V_{pv3} \\ V_{pv4} \end{bmatrix} = \begin{bmatrix} 1 & 0 & 0 & 0 & 1 \\ 0 & 0 & 0 & 1 & 1 \\ 0 & 0 & 0 & 0 & 1 \\ 0 & 0 & 1 & 1 & 1 \\ 1 & 1 & 0 & 0 & 1 \end{bmatrix} \begin{bmatrix} V_0 \\ V_1 \\ V_2 \\ V_3 \\ V_4 \end{bmatrix}$$

Ones in the voltage coefficient matrix, $\mathbf{A}$, indicate locations at which the switch did not bypass any module, and zeros are locations at which the switch did bypass the module. To find the voltage for each module in the string, as the voltage coefficient matrix $\mathbf{A}$ is square matrix, the inverse can be used as in (9).

$$\mathbf{V} = A^{-1} V_{pv} \tag{9}$$

$$\begin{bmatrix} V_0 \\ V_1 \\ V_2 \\ V_3 \\ V_4 \end{bmatrix} = \begin{bmatrix} 1 & 0 & -1 & 0 & 0 \\ -1 & 0 & 0 & 0 & 1 \\ 0 & -1 & 0 & 1 & 0 \\ 0 & 1 & -1 & 0 & 0 \\ 0 & 0 & 1 & 0 & 0 \end{bmatrix} \begin{bmatrix} V_{pv0} \\ V_{pv1} \\ V_{pv2} \\ V_{pv3} \\ V_{pv4} \end{bmatrix}$$

The result obtained from applying the matrix multiplication is as follows:

$$\begin{aligned} V_0 &= V_{pv0} - V_{pv2} \\ V_1 &= V_{pv4} - V_{pv0} \\ V_2 &= V_{pv3} - V_{pv1} \\ V_3 &= V_{pv1} - V_{pv2} \\ V_4 &= V_{pv2} \end{aligned} \tag{10}$$

These equations can be used to determine the voltage of each module in that string. Once the voltage of each module is identified, the faulty modules are detected by having a voltage below the specified module voltage threshold. Compared to the literature, our method minimizes both the number of voltage sensors and switches required to localize faults to the module level. Table II shows a summary of voltage-based fault localization techniques in comparison to our proposed method for a 10 x 10 PV system.

TABLE II
COMPARISON WITH THE OTHER EXISTING METHODS FOR 10 X 10 PV SYSTEM

Ref	Year	Components		
		Voltage Sensors	Switches	Module Level
[24]	2018	100	–	Yes
[27]	2021	5	–	No
[28]	2023	50	–	Yes
[30]	2023	1	100	Yes
Our Work	**2023**	**1**	**50**	**Yes**

Our proposed method reduces the number of switches by 50%, and can localize the fault to the module level using only one voltage sensor. In our work, the string sampling switches in the gearbox were ignored; however, if considered, our method would still minimize the switches by 40%, outperforming the work in the literature. In the next section, the theoretical analysis is employed in the simulation to examine the technique ability in faults localization.

IV. SIMULATION RESULTS

In this section, the simulation results obtained from simulating a 5 by 4 PV system shown in Fig. 5 is discussed. In the simulation, the Perturb and Observe (P&O) algorithm is used for MPPT tracking, with a sampling frequency of 8 kHz. A set of three switches is connected per string to provide an alternative path for module isolation. It is worth noting that even if the system is 6 by 4, the number of switches in the system does not change. Moreover, during a power drop, the

system is momentarily disconnected to identify which string is faulty. The system is disconnected to avoid the MPPT from becoming stuck at a local minimum. Details regarding the module specifications at Standard Test Conditions (STC) are in Table III.

TABLE III
SIMULATION MODULE SPECIFICATIONS

Parameter	Value
Maximum Power (Pmax)	213.15 W
Open Circuit Voltage (Voc)	36.3 V
Short Circuit Current (Isc)	7.35 A
Voltage at Maximum Power Point (Vmp)	29 V

A. String Level Localization

In this part, the string's voltage is sampled at fixed time intervals. Fig. 6 shows the transient response of the PV system with (P&O) MPPT during a fault. The fault is introduced into the system by shorting a module in the first string after 0.11 seconds.

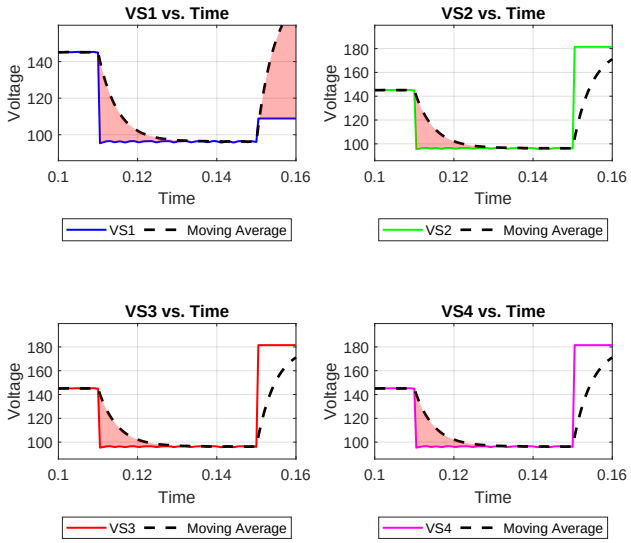

Fig. 6. String Voltage Transient Fault Response

The expected response after introducing the fault is that one of the strings would have a voltage lower than the other strings. However, the MPPT algorithm caused all voltages to drop due to getting stuck in a local minimum. Consequently, the string fault localization algorithm identified all strings as faulty. After 0.15 seconds, the power is disconnected for 1 second, leading to the identification of the first string as faulty. Therefore, to localize the faulty string, either the system is disconnected, or is operated at its maximum power point.

B. Module Level Fault Localization

Once the faulty string is localized, the first string in this case, the set of switches on that string is used to identify which modules are affected by the fault. In this part, scenarios such as line-to-line, line-to-ground, inter-string, open and partial shading faults are introduced to the string to demonstrate the technique's ability to localize faults to the module level.

1) Line-to-Line & Line-to-Ground Faults: The line-to-line fault is introduced to the string by connecting a wire between either a single or multiple modules. Similarly for a line-to-ground fault, by creating a direct connection to the ground, multiple modules gets shorted as a result. The shorted modules for each scenario, along with each voltage obtained from controlling different switch combinations are shown in Table IV.

TABLE IV
STRING VOLTAGE IN LINE-TO-LINE FAULT SCENARIOS

Scenario	**1**	**2**	**3**	**4**	**5**
Module	No Fault	03	02, 03	00, 02, 04	01, 02, 03, 04
Voc (V)	181	145	109	72	36
Vpv0 (V)	73	72	72	0	36
Vpv1 (V)	73	37	36	36	0
Vpv2 (V)	36	36	36	0	0
Vpv3 (V)	108	72	36	36	1
Vpv4 (V)	108	72	72	36	36

It can be observed that the open-circuit voltage of the string deviates from the ideal non-faulted case with each fault scenario. To gain a better understanding of the data presented in Table IV, the voltage contribution of each module can be found using (10), as depicted in Table V.

TABLE V
MODULE VOLTAGE IN LINE-TO-LINE FAULT SCENARIOS

Case	**1**	**2**	**3**	**4**	**5**
Module	No Fault	03	02, 03	00, 02, 04	01, 02, 03, 04
V00 (V)	37	36	36	**0**	36
V01 (V)	35	36	36	36	**0**
V02 (V)	35	35	**0**	**0**	**1**
V03 (V)	35	**0**	**0**	36	**0**
V04 (V)	36	36	36	**0**	**0**

As this fault is introduced by connecting a wire between each module's terminals, it can be observed that the voltage corresponding to the faulty module shows approximately zero voltage difference. For example, in the first scenario, the third module was shorted, and hence, the voltage difference across module 03 is zero. In all scenarios, shorting a module results in a corresponding zero voltage in the voltage table, and therefore, a fault location.

2) Inter-String fault: A connection is established between Module 02 and Module 13 in the second string. Voltages associated with the inter-string fault are summarized in Table VI.

TABLE VI
STRING VOLTAGE IN INTER-STRING FAULT

String	0	1
Voc (V)	154	190
Vpv0 (V)	73	72
Vpv1 (V)	72	73
Vpv2 (V)	36	36
Vpv3 (V)	81	117
Vpv4 (V)	108	108

Similarly, by using equations from (10) and the data shown in Table. VII, the voltage of each module can be determined.

TABLE VII
MODULE VOLTAGE IN INTER-STRING FAULT

String	0	1
V00 (V)	37	36
V01 (V)	35	36
V02 (V)	**9**	44
V03 (V)	35	35
V04 (V)	36	36

Due to the voltage mismatch, it can be observed that the third module in the first string experiences a significant voltage drop, and hence, is the fault location.

C. Open, and Partial Shading Fault

During an open or partial shading fault, the faulty modules are bypassed by the diode. The positive terminal of module 02 is disconnected, and the obtained string sampled voltages due to each switch combination are shown in Table. VIII

TABLE VIII
STRING VOLTAGE IN OPEN FAULT

Case	Open Circuit
Voc (V)	145
Vpv0 (V)	73
Vpv1 (V)	72
Vpv2 (V)	36
Vpv3 (V)	72
Vpv4 (V)	108

Using these samples, the voltage of each module can be found using (10) as shown in Table. IX.

TABLE IX
MODULE VOLTAGE IN OPEN FAULT

String	0
V00 (V)	37
V01 (V)	35
V02 (V)	**0**
V03 (V)	35
V04 (V)	36

It can be noticed that the voltage across the third module is zero, which is due to the usage of an ideal diode during simulation. Otherwise, under normal conditions, the voltage across the third module should be the diode forward voltage. In the next part, the experimental results for the fault detection and localization technique is presented.

V. EXPIRMENTAL RESULTS

In this section, the experimental results obtained from the setup shown in Fig. 7 is discussed. The experimental setup consists of a 300W grid-tied inverter, a PV system with the same configuration as in Fig. 5, and a multimeter. A bypass diode is connected to each module in the 5 x 4 pv system, with a blocking diode at each string to prevent reverse current flow and to disconnect the faulty string during module fault.

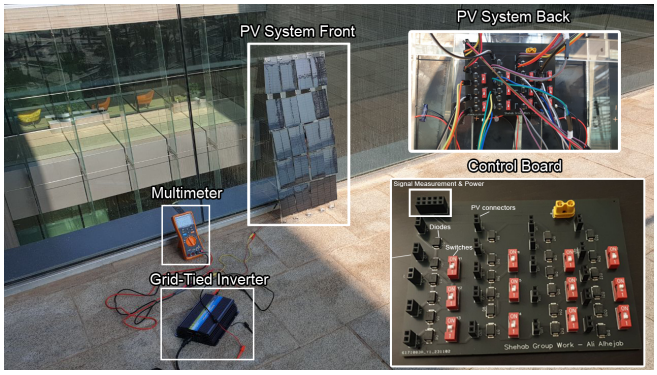

Fig. 7. Experimental Setup for Fault Detection and Localization in PV Systems

The experiment is conducted by first connecting the PV system to the grid-tied inverter, and once there is a power drop, the system gets disconnected momentarily to identify the faulty modules in the system. As mentioned earlier, the disconnection of the PV system is not necessary if the MPPT algorithm is capable of identifying the GMPP as the diode would disconnect the faulty string. However, in this part the system is disconnected right after a fault is detected. Parameters of the used experimental modules are shown in Table. X.

TABLE X
EXPERIMENTAL MODULE SPECIFICATIONS

Parameter	**Value**
Maximum Power (Pmax)	1.5 W
Open Circuit Voltage (Voc)	8.2.3 V
Voltage at Maximum Power Point (Vmp)	6.4 V
Current at Maximum Power Point (Imp)	270 mA

A. Localizing the Faulty String

In this part, the string voltage is measured after the fault is detected, and the system is disconnected. The string voltage measurement data is shown in Table. XI.

TABLE XI
STRING VOLTAGE AFTER FAULT

String	0	1	2	3
Voc	32	25.6	32	32

The second string shows a clear voltage deviation from the other strings, identifying it as a faulty string. Also, the magnitude of the fault increases with the number of faulty modules, making such differences more noticeable. The detected faulty string can be further investigated using the switches attached to that string to localize the exact location of the faulty modules.

B. Localizing Faulty Modules in a String

Once the faulty string is localized, mechanical switches are used to identify the exact location of the faulty module. A line-to-line, inter-string, and open circuit fault are introduced to see their effect on the string voltage. The string voltage is sampled using a multimeter with every different switch combination.

1) Line to Line Fault: The line-to-line fault is introduced into the system by shorting one module at a time. Table XII shows the voltage associated with each module fault scenario.

TABLE XII
STRING VOLTAGE IN LINE-TO-LINE FAULT SCENARIOS

Scenario	**1**	**2**	**3**	**4**
Module	No Fault	01	01 03	01 03 05
Voc (V)	32	25.6	18.18	12.8
Vpv0 (V)	13	6.7	6.7	0
Vpv1 (V)	13	13	12.2	6.3
Vpv2 (V)	6.3	6.3	6.3	0
Vpv3 (V)	18.8	19.3	12.5	6.3
Vpv4 (V)	18.8	12.7	12.5	6.3

Using (10), and the sampled string voltage with each switch combination, the voltage for each module is shown in Table. XIII.

TABLE XIII
MODULE VOLTAGE IN LINE-TO-LINE FAULT SCENARIOS

Case	**1**	**2**	**3**	**4**
Module	No Fault	00	00 02	00 02 04
V00 (V)	6.7	**0**	**0**	**0**
V01 (V)	5.8	6	5.8	6.3
V02 (V)	5.8	6.3	**0**	**0**
V03 (V)	6.7	6.7	5.9	6.3
V04 (V)	6.3	6.3	6.3	**0**

The zeros in the table represent the locations at which a wire is connected between the positive and negative terminals of the module, therefore shorting its two terminals.

2) Inter-String Fault: The inter-string fault is introduced by connecting a line between the second and third string. The line connectes Module 13 in the second string with Module 24 in the third string. This resulted in a voltage mismatch, hence a voltage drop in the second string, whereas the voltage in the third string remained the same. Table. XIV shows the sampled string voltage for the inter-string fault.

TABLE XIV
STRING VOLTAGE IN INTER-STRING FAULT

Case	Inter-String Fault
Voc (V)	25.6
Vpv0 (V)	12.8
Vpv1 (V)	12.7
Vpv2 (V)	6.5
Vpv3 (V)	13
Vpv4 (V)	18.5
Vpv5 (V)	18.6

Using (10), each module voltage for the inter-string fault is shown in Table. XV. The voltage across the third module is approximately zero, which mean that an unwanted connection is located at that module. Additionally, a voltage of 0.3V is calculated across the third module, indicating that the bypass diode is triggered.

TABLE XV
MODULE VOLTAGE IN INTER-STRING FAULT

String	0
V10 (V)	6.3
V11 (V)	5.7
V12 (V)	**0.3**
V13 (V)	6.2
V14 (V)	6.5

3) Open and Partial Shading Fault: The open fault is introduced by disconnecting or having a shaded module, causing the bypass diode to be triggered. For this part, the second module in the second string is disconnected, and the associated voltage measurements are shown in Table XVI. The

TABLE XVI
STRING VOLTAGE IN OPEN FAULT

Case	Open Fault
Voc (V)	25.6
Vpv0 (V)	12.5
Vpv1 (V)	13.2
Vpv2 (V)	6.3
Vpv3 (V)	19
Vpv4 (V)	19.2
Vpv5 (V)	12.7

voltage of each module using equation (10) is depicted in Table. XVII

TABLE XVII
MODULE VOLTAGE IN OPEN FAULT

String	0
V10 (V)	6.2
V11 (V)	**0.3**
V12 (V)	5.8
V13 (V)	6.8
V14 (V)	6.3

The second module exhibits a voltage of 0.3V, which is approximately the voltage of the diode at forward bias, hence, a fault is localized in that module. In both simulation and experimental conditions, the fault localization methods on line-to-line, line-to-ground, inter-string, and open circuit faults proved to be effective in localizing the fault to the module level. The string localization algorithm is a key for the module level localization to be effective. Once the string is localized, the faulty modules can be identified based on their voltage levels.

VI. CONCLUSION

In conclusion, faults in PV system can cause critical damage to the system. An easy, and cost effective technique is necessary to detect and localize these faults to the module level. Our method is switch based, and cost effective technique that minimizes the voltage sensors to one. The method proved effectiveness on line-to-line, line-to-ground, inter-string , and open faults on both simulation, and experimental setup. Future work could involve improving the speed at which faults are

detected and minimizing computation to precisely localize the faulty module.

ACKNOWLEDGMENT

The authors would like to thank Muhammad Zeeshan, an MS/PhD student at KAUST, for helping in the experimental setup.

REFERENCES

[1] M. K. Alam, F. Khan, J. Johnson, and J. Flicker, "A comprehensive review of catastrophic faults in pv arrays: Types, detection, and mitigation techniques," *IEEE Journal of Photovoltaics*, vol. 5, no. 3, pp. 982–997, 2015.

[2] P. B. Quater, F. Grimaccia, S. Leva, M. Mussetta, and M. Aghaei, "Light unmanned aerial vehicles (uavs) for cooperative inspection of pv plants," *IEEE Journal of Photovoltaics*, vol. 4, no. 4, pp. 1107–1113, 2014.

[3] S. Leva, M. Aghaei, and F. Grimaccia, "Pv power plant inspection by uas: Correlation between altitude and detection of defects on pv modules," in *2015 IEEE 15th International Conference on Environment and Electrical Engineering (EEEIC)*, 2015, pp. 1921–1926.

[4] M. Aghaei, A. Dolara, S. Leva, and F. Grimaccia, "Image resolution and defects detection in pv inspection by unmanned technologies," in *2016 IEEE Power and Energy Society General Meeting (PESGM)*, 2016, pp. 1–5.

[5] Y. Hu, W. Cao, J. Ma, S. J. Finney, and D. Li, "Identifying pv module mismatch faults by a thermography-based temperature distribution analysis," *IEEE Transactions on Device and Materials Reliability*, vol. 14, no. 4, pp. 951–960, 2014.

[6] M. Alsafasfeh, I. Abdel-Qader, and B. Bazuin, "Fault detection in photovoltaic system using slic and thermal images," in *2017 8th International Conference on Information Technology (ICIT)*, 2017, pp. 672–676.

[7] V. S. Bharath. Kurukuru, A. Haque, and M. A. Khan, "Fault classification for photovoltaic modules using thermography and image processing," in *2019 IEEE Industry Applications Society Annual Meeting*, 2019, pp. 1–6.

[8] M. Alajmi, K. Awedat, M. S. Aldeen, and S. Alwagdani, "Ir thermal image analysis: An efficient algorithm for accurate hot-spot fault detection and localization in solar photovoltaic systems," in *2019 IEEE International Conference on Electro Information Technology (EIT)*, 2019, pp. 162–168.

[9] U. K. Phoolwani, T. Sharma, A. Singh, and S. K. Gawre, "Iot based solar panel analysis using thermal imaging," in *2020 IEEE International Students' Conference on Electrical,Electronics and Computer Science (SCEECS)*, 2020, pp. 1–5.

[10] X. Li, W. Li, Q. Yang, W. Yan, and A. Y. Zomaya, "Edge-computing-enabled unmanned module defect detection and diagnosis system for large-scale photovoltaic plants," *IEEE Internet of Things Journal*, vol. 7, no. 10, pp. 9651–9663, 2020.

[11] A. K. V. de Oliveira, M. K. Bracht, A. P. Melo, R. Lamberts, and R. Rüther, "Evaluation of faults in a photovoltaic power plant using orthomosaics based on aerial infrared thermography," in *2021 IEEE 48th Photovoltaic Specialists Conference (PVSC)*, 2021, pp. 2604–2610.

[12] C. Scognamillo, A. P. Catalano, P. Guerriero, S. Daliento, L. Codecasa, and V. d'Alessandro, "Pv fault detection through ir thermography: using emphasis under uneven environmental conditions," in *2021 27th International Workshop on Thermal Investigations of ICs and Systems (THERMINIC)*, 2021, pp. 1–4.

[13] P. Zhang, Z. Zhu, T. Zheng, and C. Zhang, "Photovoltaic hot spot fault warning and treatment method based on image processing," in *2022 4th International Conference on Smart Power & Internet Energy Systems (SPIES)*, 2022, pp. 2339–2343.

[14] M. Sander, B. Henke, S. Schweizer, M. Ebert, and J. Bagdahn, "Pv module defect detection by combination of mechanical and electrical analysis methods," in *2010 35th IEEE Photovoltaic Specialists Conference*, 2010, pp. 001 765–001 769.

[15] M. Schütze, M. Junghänel, M. B. Koentopp, S. Cwikla, S. Friedrich, J. W. Müller, and P. Wawer, "Laboratory study of potential induced degradation of silicon photovoltaic modules," in *2011 37th IEEE Photovoltaic Specialists Conference*, 2011, pp. 000 821–000 826.

[16] R. Ebner, B. Kubicek, and G. Újvári, "Non-destructive techniques for quality control of pv modules: Infrared thermography, electro- and photoluminescence imaging," in *IECON 2013 - 39th Annual Conference of the IEEE Industrial Electronics Society*, 2013, pp. 8104–8109.

[17] T. Fuyuki, T. Tomimoto, A. Tani, and Y. Ishikawa, "On-site detection of defective panels in mega solar systems by handy electroluminescence surveillance," in *2015 IEEE 42nd Photovoltaic Specialist Conference (PVSC)*, 2015, pp. 1–3.

[18] A. Dolara, G. C. Lazaroiu, S. Leva, G. Manzolini, and L. Votta, "Snail trails and cell microcrack impact on pv module maximum power and energy production," *IEEE Journal of Photovoltaics*, vol. 6, no. 5, pp. 1269–1277, 2016.

[19] H. R. Parikh, S. Spataru, D. Sera, C. Mantel, S. Forchhammer, G. A. dos Reis Benatto, N. Riedel, and P. B. Poulsen, "Enhancement of electroluminescence images for fault detection in photovoltaic panels," in *2018 IEEE 7th World Conference on Photovoltaic Energy Conversion (WCPEC) (A Joint Conference of 45th IEEE PVSC, 28th PVSEC & 34th EU PVSEC)*, 2018, pp. 0447–0452.

[20] A. K. Vidal de Oliveira, C. Bedin, G. X. de Andrade Pinto, A. Mendes Ferreira Gomes, G. H. Souza Reis, L. Rafael do Nascimento, and R. Rüther, "Low-cost aerial electroluminescence (ael) of pv power plants," in *2019 IEEE 46th Photovoltaic Specialists Conference (PVSC)*, 2019, pp. 0532–0537.

[21] S. Roy, M. K. Alam, F. Khan, J. Johnson, and J. Flicker, "An irradiance-independent, robust ground-fault detection scheme for pv arrays based on spread spectrum time-domain reflectometry (sstdr)," *IEEE Transactions on Power Electronics*, vol. 33, no. 8, pp. 7046–7057, 2018.

[22] K. A. Saleh, A. Hooshyar, E. F. El-Saadany, and H. H. Zeineldin, "Voltage-based protection scheme for faults within utility-scale photovoltaic arrays," *IEEE Transactions on Smart Grid*, vol. 9, no. 5, pp. 4367–4382, 2018.

[23] L. Chen, S. Li, and X. Wang, "Quickest fault detection in photovoltaic systems," *IEEE Transactions on Smart Grid*, vol. 9, no. 3, pp. 1835–1847, 2018.

[24] L. Chen and X. Wang, "Adaptive fault localization in photovoltaic systems," *IEEE Transactions on Smart Grid*, vol. 9, no. 6, pp. 6752–6763, 2018.

[25] S. R. Madeti and S. Singh, "Online fault detection and the economic analysis of grid-connected photovoltaic systems," *Energy*, vol. 134, pp. 121–135, 2017. [Online]. Available: https://www.sciencedirect.com/science/article/pii/S0360544217309970

[26] S. Ansari, H. Samet, and T. Ghanbari, "Fault location in solar farms," *IEEE Systems Journal*, vol. 15, no. 3, pp. 4003–4012, 2021.

[27] B. P. Kumar, D. S. Pillai, N. Rajasekar, M. Chakkarapani, and G. S. Ilango, "Identification and localization of array faults with optimized placement of voltage sensors in a pv system," *IEEE Transactions on Industrial Electronics*, vol. 68, no. 7, pp. 5921–5931, 2021.

[28] W. Miao, Y. Luo, F. Wang, and C. Jiang, "Fault detection and location algorithm by voltage characteristics for pv system," *IEEE Journal of Photovoltaics*, pp. 1–11, 2023.

[29] A. Mehmood, H. A. Sher, A. F. Murtaza, and K. Al-Haddad, "A diode-based fault detection, classification, and localization method for photovoltaic array," *IEEE Transactions on Instrumentation and Measurement*, vol. 70, pp. 1–12, 2021.

[30] S. S. Sakthivel, V. Arunachalam, and K. Jagatheesan, "Detection, classification, and location of open-circuit and short-circuit faults in solar photovoltaic array: An approach using single sensor," *IEEE Journal of Photovoltaics*, pp. 1–5, 2023.